Assessment of vibration modulated regional cerebral blood flow with MRI

Linghan Kong [a,b,j,1], Suhao Qiu [a,b,j,1], Yu Chen [a,b,j], Zhao He [a,b,j], Peiyu Huang [c], Qiang He [d], Ru-Yuan Zhang [e,f], Xi-Qiao Feng [g], Linhong Deng [h], Yao Li [a], Fuhua Yan [i], Guang-Zhong Yang [a,b,j,*], Yuan Feng [a,b,i,j,*]

[a] School of Biomedical Engineering, Shanghai Jiao Tong University, Shanghai, China
[b] Institute of Medical Robotics, Shanghai Jiao Tong University, Shanghai, China
[c] Department of Radiology, The Second Affiliated Hospital, Zhejiang University School of Medicine, 310000, Hangzhou, China
[d] Shanghai United Imaging Healthcare Co Ltd, Shanghai, China
[e] Institute of Psychology and Behavioral Science, Antai College of Economics and Management, Shanghai Jiao Tong University, Shanghai, China
[f] Shanghai Mental Health Center Shanghai, School of Medicine, Shanghai Jiao Tong University, Shanghai, China
[g] Institute of Biomechanics and Medical Engineering, Department of Engineering Mechanics, Tsinghua University, Beijing, China
[h] Institute of Biomedical Engineering and Health Sciences, Changzhou University, Changzhou, Jiangsu 213164, China
[i] Department of Radiology, Ruijin Hospital, Shanghai, China
[j] National Engineering Research Center of Advanced Magnetic Resonance Technologies for Diagnosis and Therapy (NERC-AMRT), Shanghai Jiao Tong University, Shanghai, China

ARTICLE INFO

ABSTRACT

Human brain experiences vibration of certain magnitude and frequency during various physical activities such as vehicle transportation and machine operation, which may cause traumatic brain injury or other brain diseases. However, the mechanisms of brain pathogenesis due to vibration are not fully elucidated due to the lack of techniques to study brain functions while applying vibration to the brain at a specific magnitude and frequency. Here, this study reported a custom-built head-worn electromagnetic actuator that applied vibration to the brain in vivo at an accurate frequency inside a magnetic resonance imaging scanner while cerebral blood flow (CBF) was acquired. Using this technique, CBF values from 45 healthy volunteers were quantitatively measured immediately following vibration at 20, 30, 40 Hz, respectively. Results showed increasingly reduced CBF with increasing frequency at multiple regions of the brain, while the size of the regions expanded. Importantly, the vibration-induced CBF reduction regions largely fell inside the brain's default mode network (DMN), with about 58 or 46% overlap at 30 or 40 Hz, respectively. These findings demonstrate that vibration as a mechanical stimulus can change strain conditions, which may induce CBF reduction in the brain with regional differences in a frequency-dependent manner. Furthermore, the overlap between vibration-induced CBF reduction regions and DMN suggested a potential relationship between external mechanical stimuli and cognitive functions.

1. Introduction

Vibration is a common mechanical stimulus to our brain during daily life and work, such as in-vehicle transportation and machine operation, which has been strongly associated with symptoms of motion sickness (Donohew and Griffin, 2004; Howarth and Griffin, 2003; Joseph and Griffin, 2007; Murdin et al., 2011; Weech et al., 2018), vibration syndrome (Chang et al., 1994), vertigo, and dizziness (Zwergal and Dieterich, 2020). In more severe cases, both short-period dynamic high impact and long-period repetitive moderate vibration can cause trau-

matic brain injury (TBI) (Asken et al., 2017; Bahrami et al., 2016; Benjamini et al., 2021; Bernick et al., 2020; Buskirk, 2019; Cloots et al., 2008; Gardner et al., 2018; Haber et al., 2021; Hirad et al., 2019; Steinman et al., 2019; Stovell et al., 2020; Tagge et al., 2018). The etiology of vibration-induced TBI, however, is not fully elucidated due to lack of knowledge about how vibration actually affects the human brain.

In studies concerning vibration-induced tissue damage in hand-arm vibration syndrome (HAVS), it has been widely observed that vibration causes an early effect of vasoconstriction that leads to obstruction of blood flow and oxygen transportation to the tissue (Bovenzi et al., 2006;

Curry et al., 2002, 2005; Hua et al., 2017; Palmer and Collin, 1993; Stoyneva et al., 2003). And the vasoconstriction has also been found to be dependent on both the magnitude and frequency of the vibration (Bovenzi et al., 2000; Ye and Griffin, 2014). On the other hand, patients with TBI also show reduced cerebral blood flow (CBF), a major physiological marker of brain functions, in the bilateral frontotemporal regions, together with structural changes of the cerebral blood vessels and disintegrity of white matter (Clark et al., 2017; Raichle, 2015; Wang et al., 2015). Widespread deficits of CBF have also been found in gray matter in correlation with severity of TBI and cognitive dysfunction (Ware et al., 2020).

Recent computational simulation studies appeared to indicate that vibration-induced effects on brain functions may well be frequency-dependent. Specifically, a study used finite element method (FEM) to computationally simulate the motion and strain for brain models based on dynamics data from injured and non-injured athletes subjected to head impacts and found that the brain was more susceptible to vibration at frequency ranging between 20 and 40 Hz, with strain peaking at around 30 Hz (Laksari et al., 2018). However, all the present imaging modalities in neuroscience prevent in vivo quantitative measurement of physiological and functional changes in the brain during vibration because the head motion is always considered an artifact and supposed to be carefully avoided during imaging or eliminated in post-hoc imaging analysis. Therefore, it remains a fundamental challenge to experimentally characterize the in vivo frequency-dependence of vibration-induced effects on brain functions despite its critical importance for understanding the mechanism of brain disease caused by vibration.

To overcome this challenge and prove our hypothesis that exposure to the vibration on the brain could reduce CBF in the brain in a region-specific and frequency-dependent fashion, a custom-built electromagnetic actuator was worn by each subject inside the MR head coil to introduce mechanical vibration to the brain at frequencies of 20, 30, and 40 Hz, respectively, and CBF was measured immediately after vibration. Using this technique, we found that vibration caused reduction of CBF, which was highly dependent on the frequency of vibration as well as the region in the brain. In particular, the regions with vibration-reduced CBF appeared to largely overlap with the brain's default mode network (DMN) associated with cognitive processes (Yeshurun et al., 2021). These findings not only prove the concept of characterizing brain functions under specific vibration conditions, but also provide an important relationship between the external mechanical stimulation and the internal CBF and cognitive functions of the human brain, which may be essential for fully understanding the pathophysiological mechanisms of brain damage due to exposure to environmental vibrations as well as potentially help developing better approaches for preventing/treating vibration-induced brain injury.

2. Material and methods

2.1. Subjects and ethical approval

Fifty-two healthy volunteers (age 25.87±2.78 years old, 31F/21 M) participated in this study. All subjects provided informed consent, as approved by the Science and Technology Ethics Committees of the Shanghai Jiao Tong University. Among all volunteers, 7 subjects' data were excluded due to motion artifacts, resulting in a total of 45 subjects (26.05±3.09 years old, 26F/19 M) for subsequent analyses.

2.2. Study design

To investigate the CBF changes after vibration, we carried out imaging in two sessions (Fig. 1): a reference session without vibration (session 1) and with vibration (session 2). Session 1 included a high-resolution T1-weighted (T1W) imaging sequence for anatomical MRI (aMRI), followed by a 3D pseudo-continuous arterial spin-labeling (pCASL) sequence to measure resting CBF (C_0). At the end of session 1, subjects

would rest for 5 min. Session 2 included 3 similar imaging modules corresponding to imaging at 3 vibration frequencies (20 Hz, 30 Hz, and 40 Hz). The excitation power of the actuator was set to 3.3 W in all frequency. The order of the measurement frequency for each module was carried out in a randomized, counterbalanced way. The vibration motion was induced using a high-frequency accuracy electromagnetic actuator (Qiu et al., 2021). The vibration amplitude of the actuator was measured by an accelerometer at 20 Hz, 30 Hz, and 40 Hz, with a magnitude of 1.97±0.15 mm, 1.62±0.11 mm, and 1.42±0.10 mm, respectively. Extensive tests have been carried out in previous studies to verify that there is no interference between the actuation and the imaging (Qiu et al., 2021). The vibration actuator stayed on the heads of the subjects for the whole experiment. It was not taken off during the rest modules. The subjects stayed inside the scanner until all the scans were finished.

At each imaging module of session 2, wave images from vibration were also acquired using a magnetic resonance elastography (MRE) sequence to characterize the in-brain displacement field of vibration at 3 frequencies. After vibration at each imaging module of session 2, CBF was measured immediately using a pCASL sequence. To ensure the reliability and repeatability of the results, the above two imaging steps were repeated for each module. The total time for both sessions was 90 min. Subjects were requested to keep their eyes open during the experiment.

Additional 10 subjects were recruited to verify post vibration if the CBF returns to baseline after 5-minute rest. The baseline regression includes 3 frequency blocks (Fig. 1c). In each block, resting-state CBF (R1, R3, R5) values were first measured 5 min before vibration. After vibration, the subjects had a 5-minute rest. Then, CBF (R2, R4, R6) values were measured again. Paired student t-tests were used to verify whether the CBF went back to the baseline between different vibrational modules (R1 vs. R2; R3 vs. R4; R5 vs. R6).

2.3. Imaging protocols

All images were acquired on a 3T MRI scanner (uMR790, United Imaging Healthcare, Shanghai, China) with a 24-channel head coil. High-resolution T1W images were acquired to cover the whole brain with a 3D gradient-echo sequence with the following parameters: TR/TE=1068.1/3.4 ms, slices=320, FOV=256 mm × 240 mm, voxel size=0.8 × 0.8 × 0.8mm³. CBF values were measured using a 3D pCASL sequence with the following parameters: 12 tag-control image pairs, 34 transversal slices, TR/TE=4702/14.14 ms, label duration=1.8 s, post-labeling delay (PLD)=1.8 s, FOV=224 mm × 224 mm, voxel size=3.5 × 3.5 × 4mm³. The CBF values were obtained by:

$$CBF = \frac{6000 \cdot \lambda \cdot \left(SI_{control} - SI_{label} \right) \cdot e^{\frac{PLD}{T_{1,blood}}}}{2 \cdot \alpha \cdot T_{1,blood} \cdot SI_{PD} \cdot \left(1 - e^{-\frac{\tau}{T_{1,blood}}} \right)} \left[\frac{ml}{\frac{100g}{min}} \right]$$

where the brain-blood water partition coefficient $\lambda = 0.9 \ mL/g$, $SI_{control}$, SI_{label} and SI_{PD} are the control, label, and proton density-weighted images, respectively, $T_{1,blood} = 1650 \ ms$ is the longitudinal relaxation time of the blood at 3T, $\alpha = 0.85$ is the labeling efficiency for pCASL, τ is the label duration.

MRE was performed during each vibration session (Qiu et al., 2021). A single-shot echo-planar imaging (EPI) based MRE sequence with a first-nulling motion encoding gradient (MEG) was used for brain displacement measurement. The MEG had a strength of 30 mT/m and the repetition/echo time (TR/TE) was 3400/71.6 ms. A total of 34 slices with a thickness of 4 mm was collected for each object. The FOV was 224 mm × 224 mm with a matrix size of 128 × 128. The principal component of the displacement fields was filtered by a 2D Gaussian filter with a kernel size of 5 × 5 pixels and a standard deviation of 0.65. The three principal strain components (ε_1, ε_2, and ε_3) and octahedral shear strain (ε_{oss}) for each frequency were calculated (McGarry et al., 2011) to explore their correlation with the changes of CBF.
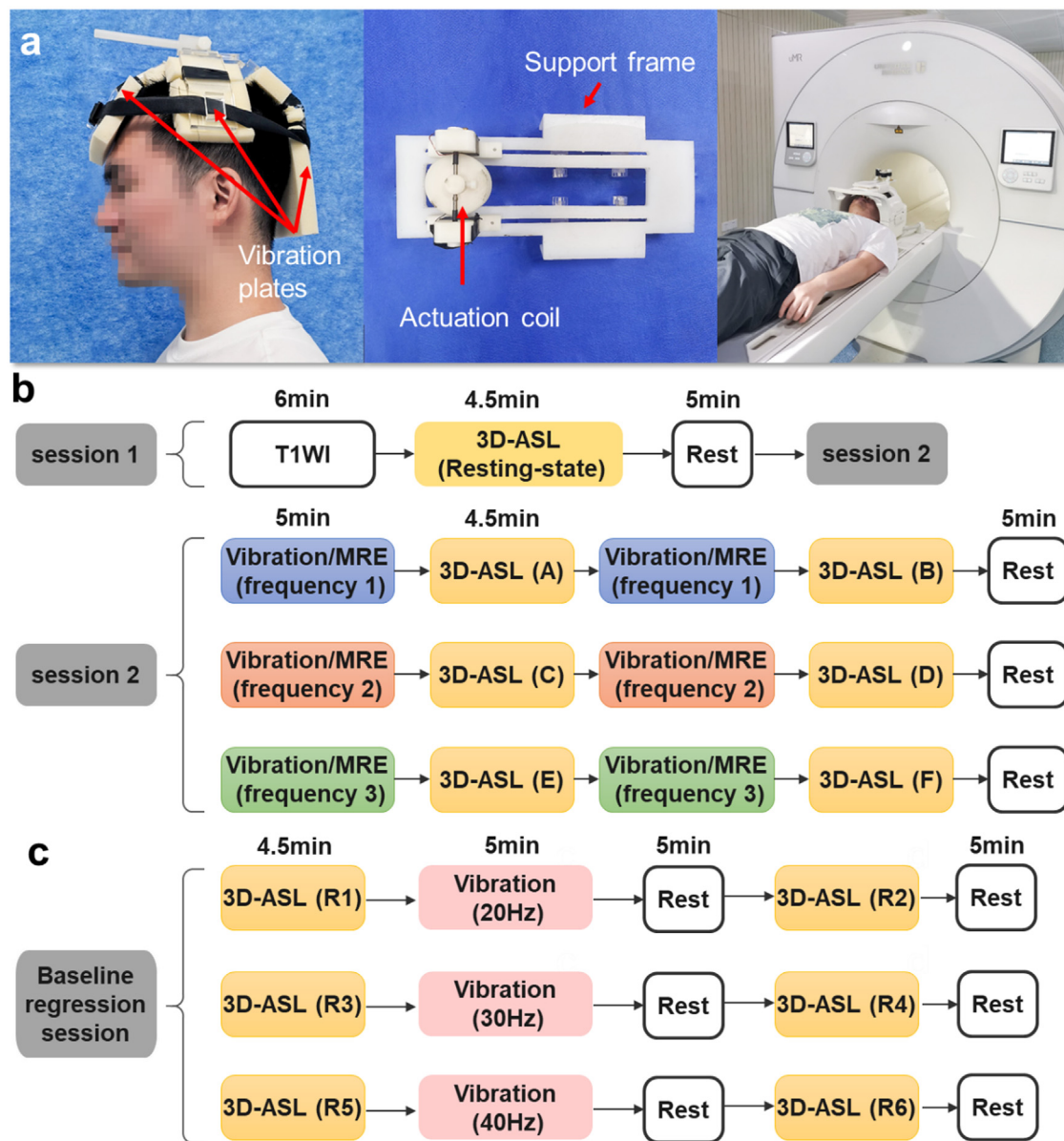
Fig. 1. Experimental set-up and procedure for measuring the vibration effect on cerebral blood flow. (a) Custom-built head worn electromagnetic vibration actuator consisting several plates that transmitted vibration to the brain. The plates were attached with soft sponge pads to ensure the scanning was comfortable. The actuator was used for both vibration actuation and MRE acquisition (Qiu et al., 2021). A supine position was adopted for all imaging procedures. (b) The imaging protocol includes two sessions. Anatomical images (T1W) and CBF maps in the absence of vibration were acquired as references in session 1. In session 2, CBF was measured immediately after the vibration using a pCASL sequence. During the vibration modules, MRE sequence were utilized to characterize the in-brain displacement field. The CBF measurements were repeated once more to ensure experimental reproducibility. The order of frequency scanning between 20, 30, 40 Hz was randomized to minimize the potential influence of sequential measurement order. (c) Baseline regression tests were designed to verify if the CBF returned to baseline after a 5-minute vibration at 20, 30, and 40 Hz. In each block, CBF maps were acquired before vibration and after the 5-minute rest.

2.4. Data analyses

First, skulls were excluded from T1W images using BET2 (Smith, 2002) from the FMRIB Software Library (Jenkinson et al., 2012; Smith et al., 2004; Woolrich et al., 2009) (FSL v6.0, Oxford center for Functional MRI of the Brain, Oxford, UK). Then, CBF maps were realigned to T1W images using SPM12 (Wellcome Trust center for Neuroimaging, London, UK,). CBF maps were resampled into 2 mm³ isotropic voxels and normalized to the anatomical standard space defined by the Montreal Neurological Institute (MNI) using Advanced Normalization Tools (ANTs) (Avants et al., 2011). Masks from the automated anatomical labeling atlas (AAL) (Tzourio-Mazoyer et al., 2002) were also used. Cortical surface ROIs defined by AAL template in MNI

space are given in the Supplement Information Table S1. CBF maps were standardized for reducing individual variance by $C_z = \frac{(C-\mu)}{\sigma}$ (Liu et al., 2016a; Pfefferbaum et al., 2011), where C_z is the standardized CBF value at each voxel, C is the original CBF value, μ and σ are the mean and standard deviation of the whole-brain CBF. Finally, images were smoothed with a Gaussian kernel of $8 \times 8 \times 8$ mm³ full width at half maximum (FWHM) by SPM12.

Significance analyses were carried out concerning the normalized CBF maps using paired student t-tests or two-sample t-tests. A two-tailed permutation test with 5000 permutations was used to find significant clusters with the tool Permutation Analysis of Linear Models (PALM) (Winkler et al., 2016), and multiple comparisons were corrected by the family-wise error rate (FWER) method with threshold-free cluster en-
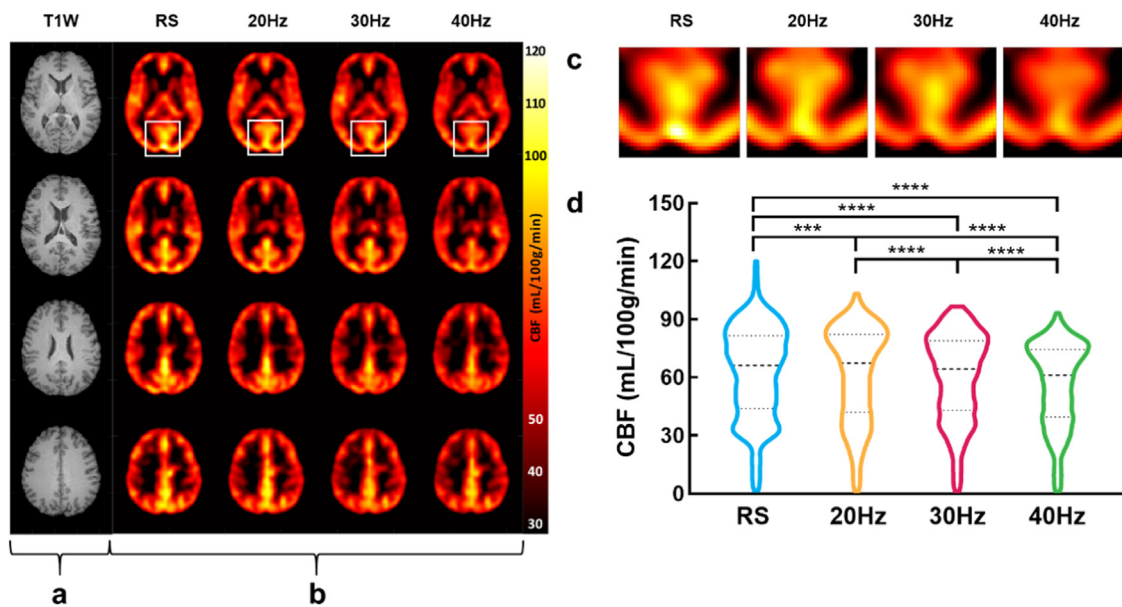
Fig. 2. Effect of vibration on cerebral blood flow with frequency dependence. (a-b) Typical anatomical images (T1W) and CBF maps of the brain acquired from one volunteer subject in the absence (resting state, RS) or presence of vibration for 5 min at different frequencies (20, 30, 40 Hz, respectively). The white rectangle box in the top row of CBF map shows an example region (PCC and PCUN). (c) Magnified view of the boxed region in the top row of CBF maps in panel a-b, showing decreasing CBF with increasing vibration frequency (RS to 40 Hz from left to right). (d) Statistical analysis results of quantitative CBF data acquired from 45 subjects, showing significant decrease of CBF in regions including PCC and PCUN after vibration was applied with increasing frequency. (RS vs. 20 Hz vs. 30 Hz vs. 40 Hz, ***: $p<0.001$; ****: $p<0.0001$).

hancement (TFCE) (Smith and Nichols, 2009). A cluster-based threshold of $Z>2.3$ was applied. The significance level was set to $p<0.05$ for the suprathreshold clusters. The cluster analyses were thresholded at $t>1.96$ or $t<-1.96$. Toolbox for Data Processing & Analysis of Brain Imaging (DPABI_V6.0 toolkit (Yan et al., 2016),) and MATLAB (MathWorks, Natick, MA, United States) was used for all statistical analysis. Then, the number of overlapped significant voxels in each brain network (MNI space) was estimated for each frequency. The percentage of overlapped significant clusters in all networks and all significant regions were also calculated respectively. In addition, paired student t-tests were made to compare the mean CBF values at the resting state and each of the vibration state at each network for all subjects.

3. Results

3.1. Vibration decreased CBF with increasing frequency

During session 1, brain anatomy (T1W images) and CBF (3D-ASL) in the absence of vibration were acquired as references. During session 2, after vibration (3D-ASL) at frequency of 20, 30, 40 Hz, CBF were immediately acquired twice. These frequencies were chosen because of their significant role in inducing TBI (Laksari et al., 2018).

Fig. 2a-b shows typical anatomical T1W images and of CBF maps measured at either the resting state (RS) or immediately after vibration at 20, 30, 40 Hz, respectively. For each frequency, the measurement of CBF were repeated twice to ensure experimental reproducibility. No significant differences were observed in any clusters at the same frequency (paired student t-tests, $p>0.05$). Therefore, the mean values of the CBF maps at the same frequency from the two repeated measurements were used for analysis. Fig. 2c shows magnified view of CBF maps in the corresponding boxed region in the top row CBF maps of Fig. 2a-b, of which the intensity appeared to be decreasing with increasing frequency. Statistical analysis results confirmed that CBF in the boxed region (posterior cingulate cortex, PCC; precuneus, PCUN) decreased significantly in the presence of vibration with increasing frequency. (Fig. 2d, paired student t-tests, RS vs. 20 Hz vs. 30 Hz vs. 40 Hz, $p<0.05$). For the baseline re-

gression session, no significant differences were observed in any clusters at each of the frequency block (R1 vs. R2, R3 vs. R4, R5 vs. R6) (paired student t-tests, $p>0.05$). These results indicate that CBF could go back to the baseline between different vibrational modules after a 5-minute rest.

3.2. Vibration with increasing frequency induced expansion of the CBF reduction regions

Fig. 3 displays in comparison the regional distribution of CBF variations either in the absence of vibration (resting state) or in the presence of vibration at frequency of 20, 30, 40 Hz, respectively (paired student t-test). Regions of interest (ROIs) showing clusters with significant group differences ($p<0.05$) were illustrated.

As compared with resting state, vibration at 20 Hz induced no significant difference in CBF in the whole brain (data not shown). However, vibration at 30 Hz versus resting state induced a significant decrease of CBF in the region of posterior cingulate cortex (PCC), precuneus (PCUN), inferior temporal gyrus (ITG), inferior parietal gyrus (IPL), angular gyrus (ANG), supramarginal gyrus (SMG), superior frontal gyrus, medial (SFGmed), middle temporal gyrus (TPOmid), superior temporal gyrus (TPOsup), precentral (PreCG), and superior frontal gyrus (SFG) ($p_{corr}<0.05$, Fig. 3a). And vibration at 40 Hz versus resting state induced a significantly decrease of CBF in the region of PCC, PCUN, ITG, IPL, ANG, SMG, SFGmed, TPOmid, TPOsup, PreCG, SFG, and middle frontal gyrus (MFG) ($p_{corr}<0.05$, Fig. 3b).

Comparing CBF maps acquired in the presence of vibration at various frequencies, we found significant differences of CBF in ROIs between vibrations at 20 Hz and 40 Hz. Specifically, the significant decrease of CBF occurred in the region of ANG, SMG, SFG, TPOmid, TPOsup, IFG, MFG, and inferior frontal gyrus, orbital (ORBinf) ($p_{corr}<0.05$, Fig. 3c). However, no significant difference of CBF was observed between the experimental group with vibration at either 30 Hz versus 40 Hz, or 20 Hz versus 30 Hz. Fig. 3d shows that the cluster size of the CBF reduction regions increased from 0 to about 1.5×10^4 as the vibration frequency increased from 20 to 40 Hz. Detailed statistics of the cluster reports are
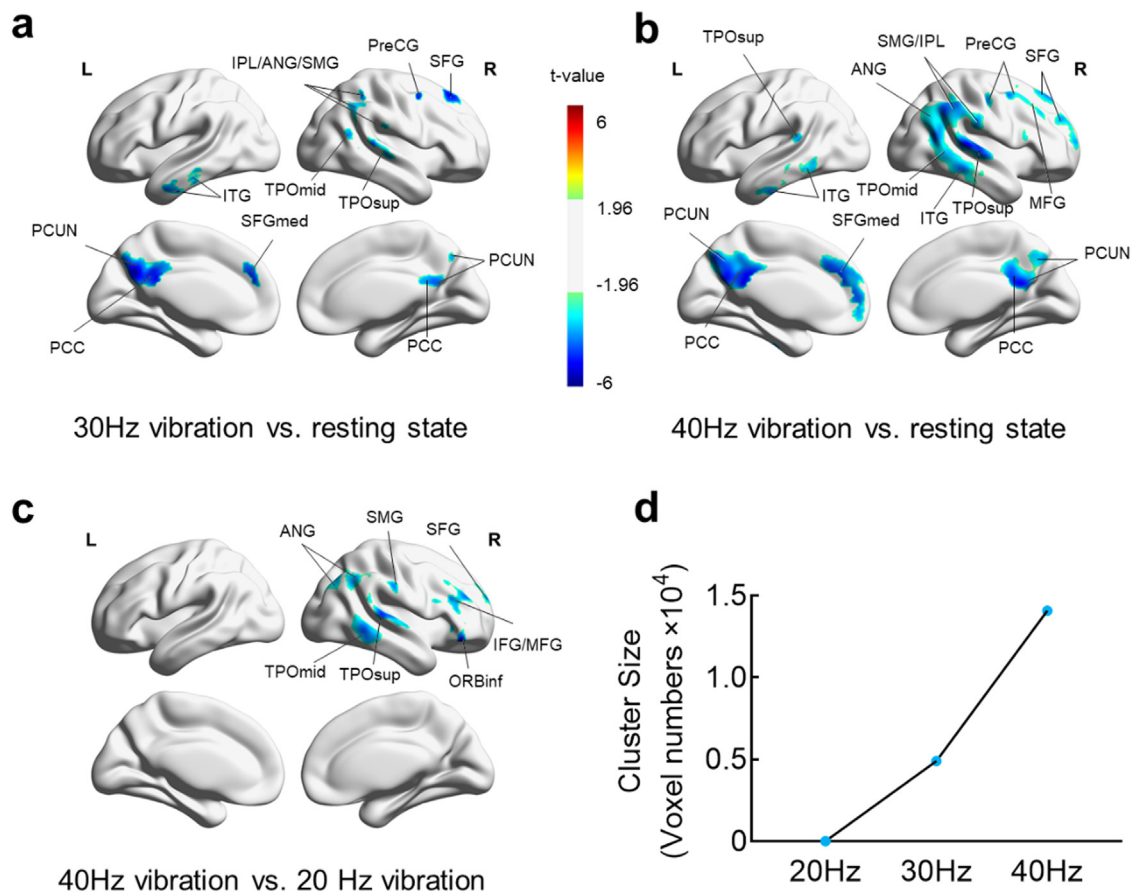
Fig. 3. Comparison of the regions with significant CBF reduction in the brain after exposure to vibration at different frequencies. (a) CBF reduction regions of the brain after 30 Hz vibration vs. resting state; (b) CBF reduction regions of the brain after 40 Hz vibration vs. resting state; (c) CBF reduction regions of the brain after 40 Hz vibration vs. 20 Hz vibration. (d) Quantified cluster size of regions with significant decrease of CBF versus vibration frequency. Note: Plots were made on the AAL brain atlas. All significant maps were corrected for permutation test and display significant voxels at $p<0.05$, ANG (angular gyrus), CUN (cuneus), IPL(inferior parietal gyrus), ITG (inferior temporal gyrus), MFG (middle frontal gyrus), ORBinf (inferior frontal gyrus, orbital), PCC (posterior cingulate cortex), PCUN (precuneus), PreCG (precentral), SFGmed (superior frontal gyrus, medial), SMG (supramarginal gyrus),TPOmid (middle temporal gyrus) TPOsup (superior temporal gyrus).

given in the Supplement Information Table S2. Furthermore, typical displacement fields and ε_{oss} at 3 frequencies were shown in Supplementary Figures S1 and S2. The mean and standard deviation of the displacement due to vibration were 13.56±2.87 μm (20 Hz), 13.01±2.97 μm (30 Hz), and 12.76±4.03 μm (40 Hz), respectively. Paired t-tests were used to compare the mean values of ε_1, ε_2, ε_3, and ε_{oss} at regions with significant CBF changes (Figs. 3a, b) across subjects for 30 Hz and 40 Hz. Significant differences were observed for ε_1 ($p<0.05$), ε_2 ($p<0.01$) and ε_{oss} ($p<0.0001$).

3.3. Vibration-induced CBF reduction regions overlapped with the brain's default mode network

To explore how CBF changes could affect brain function, we compared the brain regions showing significant CBF reduction with the 7 brain networks known for cognitive functional connectivity (Yeo et al., 2011). The number of overlapping voxels between the regions with significant CBF reduction and those in each of the 7 brain network was estimated for each frequency. We found a large overlap between the regions with significant CBF reduction and the Default Mode Network (DMN) in the brain after vibration at either 30 Hz (Fig. 4a) or 40 Hz (Fig. 4b). Quantitatively, 58% of voxels in the significant region were in DMN, accounting for 9.03% of DMN in the brain after vibration at 30 Hz (Fig. 4c), and 45.64% of voxels in the significant CBF reduction

region were in DMN, accounting for 20.02% of DMN in the brain after vibration at 40 Hz (Fig. 4d). Detailed statistics of the overlapped significant CBF reduction regions are shown in Supplement Information Table S3.

In addition, we calculated the mean CBF at each network for all subjects after vibration to the brain at each frequency. Paired student t-tests showed no significant differences of CBF in each network between each vibration frequency (Supplement Information Figure S3), but CBF in the subregions (PCC.L and ACG.R) in DMN was significantly different after vibration at different frequency (Supplement Information Figure S4), possibly due to the average effects of CBF in DMN.

4. Discussions

Physical stimuli of our head in daily life are remarkably diverse, posing great challenges to the understanding brain functions across physical conditions. A vibration is a common form of head motion. Elucidating the effects of vibration on brain functions not only expands our understanding of the basic science of the brain, but also provides new evidence for the mechanism of vibration-induced brain injury. In this study, we investigated the effects of brain vibration on CBF at three different frequencies that are known to be associated with brain injury. We found that compared to the resting state, dynamic vibration that produces oscillating displacement and changes of strain distributions (Supplement
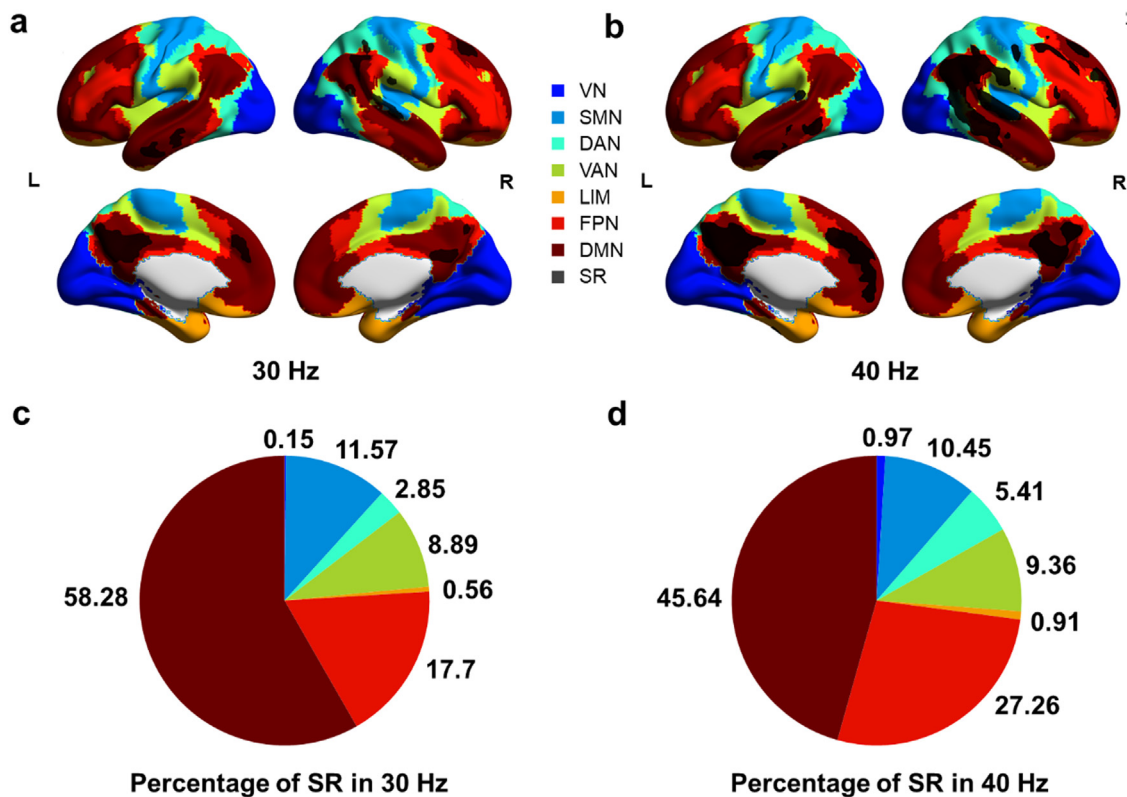
Fig. 4. Overlap of the regions with significant reduction of CBF after vibration with the seven brain functional connectivity networks. (a-b) Voxels in regions with significant CBF reduction (SR) after vibration at 30 Hz, 40 Hz, respectively, were overlaid with the seven functional connectivity networks of the brain. (c-d) Pie charts of the percentage of voxels in the significant CBF reduction region that overlapped with the seven brain networks after vibration at 30 Hz, 40 Hz, respectively. Note: The significant CBF reduction mainly happened within DMN, VN (Visual Network), SMN (Sensory-Motor Network), DAN (Dorsal Attention Network), VAN (Ventral Attention Network), LIM (Limbic), FPN (Frontoparietal Network), DMN (Default Mode Network), SR (Significant CBF Reduction Regions).

Information Figure S1 and Figure S2) could induce distinct regional reduction of CBF, which was frequency-dependent, i.e., the regions with CBF reductions showed progressively lower CBF at increasing frequency of the vibration. This finding is consistent with that vibration causes an early effect of vasoconstriction in HAVS, which is frequency-dependent (Bovenzi et al., 2000; Ye and Griffin, 2014). We also found that the regions with significant CBF reduction after vibration fell inside DMN that is associated with the brain's cognitive functional connectivity.

Previous studies have shown that CBF can be reduced significantly after brain injury in cases such as mild TBI and sports-related concussion (Churchill et al., 2017; Ge et al., 2009; Lin et al., 2016; Meier et al., 2015; Peng et al., 2016; Wang et al., 2019). Our finding of significant CBF reduction after vibration was consistent with those clinical observations. The method reported in the present study suggests that the vibration-based quantitative measurement technique has the potential to simulate impact and vibration to the human brain while accessing the physiological responses of the brain. Therefore, this method may be very useful for investigation of various vibration-induced brain diseases.

Furthermore, we found in this study that the regions with significant CBF reduction were mainly located in PCC and PCUN within DMN. These regions are known to be associated with attention, memory, perception, action, and cognition (Gordon et al., 2020; Liang et al., 2013; Raichle, 2015; Warren et al., 2014; Yu et al., 2019). Such close relationship between the brain regions that responded to vibration by changing CBF and those associated with cognitive functions provides tangible clues to explain why people feel tired after staying in a working condition with vibrations such as riding in car or operating a percussion drill. These results are also in line with other studies concerning CBF and brain functions of TBI patients. For example, a study showed evidence

for increased cerebrovascular reactivity and function connectivity in the medial regions of the DMN in college athletes experienced concussion (Militana et al., 2016). Another study reported that the first 5-mins psychomotor vigilance task decreased the CBF of mild TBI patients in the acute phase in DMN areas (Liu et al., 2016b).

To understand the effect of vibration on cognitive resources, N-back tests (Gevins and Cutillo, 1993; Owen et al., 2005) were carried out to evaluate the changes of cognitive resource based on working memory. The test protocol was explained in detail in supplements. Results showed that vibration as a physical stimulation could induce alteration of the cognitive resources. Studies have already showed neural activity was related with CBF changes (Buxton, 2021; Claassen et al., 2021; Jones et al., 2004). As one of the limitations of this study, the role of cognitive resources was not investigated here, but merits a future study. Therefore, our results bring attention to the fact that vibration as a physical stimulation may induce cognition, memory, or action-related changes.

Our finding of the frequency-dependence of CBF reduction due to vibration has many implications. In the experiments with vibration at frequency of 20, 30, 40 Hz, the size of the regions with significant CBF reduction consecutively expanded when the frequency exceeded 20 Hz. Although we did not test it, we speculated a consistent trend of expanding CBF reduction regions as the frequency further increased. This indicated that in an environment with vibration, absorption or damping for vibration at frequency over 20 Hz is desired to protect the brain. Compared with computational studies that showed peak strain in the brain exposed to vibration at 30 Hz, our results indicated that during an impact, the brain might respond by varying CBF in different patterns. Moreover, the fact that CBF reduction in specific regions such as PCC and PCUN in a frequency-dependent fashion may open a new door

for using physical modulation of CBF with external vibration as a therapeutic approach to treat certain brain regions. Another indication of our results is that the vibration may influence the measurements of CBF or other perfusion-related values. Therefore, in terms of measurement order, it is suggested that CBF or BOLD-fMRI tests be carried out before applying any physical stimulation to the brain. We observed that CBF changes with strain, and the strain values of 40 Hz were significantly higher than that of 30 Hz, with ε_{oss} showing the most significant differences (Supplementary Figure S5). Future work includes further clarification of the role of strain in affecting CBF changes, and investigation of the interrelationship between frequency, strain, and CBF in patients.

The limitations of this study were: (1) Only three frequencies were investigated due to the allowable scan time; (2) Considering the limit of scan time, a single delay pCASL sequence was used with PLD=1800 ms (Alsop et al., 2015), which may be improved with muti-PLD pCASL to improve the quantification of CBF; (3) Considering the intrinsically low SNR of ASL, to avoid the potential caveat of statistical effect, future work should consider other reference techniques such as positron emission computed tomography (PET) to measure the CBF changes after vibration to verify the effect reported. (4) Only N-back tests were used to assess the cognitive changes after vibration in a preliminary way, no detailed behavioral and cognitive changes were investigated. In future study, the protocol for human model studies should be further improved and also expanded to include patients with mild TBI or depression. It should also be studied the delicate application of vibration with respect to specific regions for accurate control of CBF modulation.

5. Conclusion

It was discovered in this study that vibration to the human brain that brings tissue strain changes caused increasing reduction of CBF with increasing vibration frequency, and the regions in which vibration modulated CBF largely overlapped with those responsible for functional connectivity. Such relationship between the vibration-induced CBF modulation and the brain functional structure provides a new way to understand the functional influences of mechanical stimuli to the human brain. And the method presented in this report can also be used to apply mechanical vibration to the human brain as a stimulus to modulate CBF in studies of various vibration-related brain diseases.

Ethics statement

The studies involving human participants were reviewed and approved by the Science and Technology Ethics Committees of the Shanghai Jiao Tong University. The patients/participants provided their written informed consent to participate in this study.

Declaration of Competing Interests

The author(s) declared no potential conflicts of interest concerning the research, authorship, and/or publication of this article.

Credit authorship contribution statement

Linghan Kong: Conceptualization, Methodology, Software, Visualization, Investigation, Formal analysis, Writing – original draft. **Suhao Qiu:** Data curation, Methodology, Software, Formal analysis, Writing – original draft. **Yu Chen:** Visualization, Software. **Zhao He:** Resources, Software. **Peiyu Huang:** Writing – review & editing. **Qiang He:** Writing – review & editing. **Ru-Yuan Zhang:** Writing – review & editing. **Xi-Qiao Feng:** Writing – review & editing. **Linhong Deng:** Writing – review & editing. **Yao Li:** Writing – review & editing. **Fuhua Yan:** Writing – review & editing. **Guang-Zhong Yang:** Conceptualization, Funding acquisition, Resources, Supervision, Writing – review & editing. **Yuan Feng:** Conceptualization, Funding acquisition, Resources, Supervision, Writing – review & editing.

Data availability

The original contributions presented in the study are included in the article/supplementary material, Further inquiries can be directed to the corresponding author(s).

Supplementary materials

Supplementary material associated with this article can be found, in the online version, at doi:10.1016/j.neuroimage.2023.119934.

References

Alsop, D.C., Detre, J.A., Golay, X., Günther, M., Hendrikse, J., Hernandez-Garcia, L., Lu, H., MacIntosh, B.J., Parkes, L.M., Smits, M., van Osch, M.J., Wang, D.J., Wong, E.C., Zaharchuk, G., 2015. Recommended implementation of arterial spin-labeled perfusion MRI for clinical applications: a consensus of the ISMRM perfusion study group and the European consortium for ASL in dementia. Magn. Reson. Med. 73, 102–116.

Asken, B.M., Sullan, M.J., DeKosky, S.T., Jaffee, M.S., Bauer, R.M., 2017. Research gaps and controversies in chronic traumatic encephalopathy: a review. JAMA Neurol. 74, 1255–1262.

Avants, B.B., Tustison, N.J., Song, G., Cook, P.A., Klein, A., Gee, J.C., 2011. A reproducible evaluation of ANTs similarity metric performance in brain image registration. Neuroimage 54, 2033–2044.

Bahrami, N., Sharma, D., Rosenthal, S., Davenport, E.M., Urban, J.E., Wagner, B., Jung, Y., Vaughan, C.G., Gioia, G.A., Stitzel, J.D., Whitlow, C.T., Maldjian, J.A., 2016. Subconcussive head impact exposure and white matter tract changes over a single season of youth football. Radiology 281, 919–926.

Benjamini, D., Iacono, D., Komlosh, M.E., Perl, D.P., Brody, D.L., Basser, P.J., 2021. Diffuse axonal injury has a characteristic multidimensional MRI signature in the human brain. Brain 144, 800–816.

Bernick, C., Shan, G., Zetterberg, H., Banks, S., Mishra, V.R., Bekris, L., Leverenz, J.B., Blennow, K., 2020. Longitudinal change in regional brain volumes with exposure to repetitive head impacts. Neurology 94, e232–e240.

Bovenzi, M., Lindsell, C.J., Griffin, M.J., 2000. Acute vascular responses to the frequency of vibration transmitted to the hand. Occup. Environ. Med. 57, 422–430.

Bovenzi, M., Welsh, A.J., Della Vedova, A., Griffin, M.J., 2006. Acute effects of force and vibration on finger blood flow. Occup. Environ. Med. 63, 84–91.

Buskirk, J.K., 2019. mTBI/Concussion. In: Neurosensory Disorders in Mild Traumatic Brain Injury, pp. 405–415.

Buxton, R.B., 2021. The thermodynamics of thinking: connections between neural activity, energy metabolism and blood flow. Philos. Trans. R. Soc. Lond. B 376, 20190624.

Chang, K.Y., Ho, S.T., Yu, H.S., 1994. Vibration induced neurophysiological and electron microscopical changes in rat peripheral nerves. Occup. Environ. Med. 51, 130–135.

Churchill, N.W., Hutchison, M.G., Richards, D., Leung, G., Graham, S.J., Schweizer, T.A., 2017. The first week after concussion: blood flow, brain function and white matter microstructure. Neuroimage Clin. 14, 480–489.

Claassen, J., Thijssen, D.H.J., Panerai, R.B., Faraci, F.M., 2021. Regulation of cerebral blood flow in humans: physiology and clinical implications of autoregulation. Physiol. Rev. 101, 1487–1559.

Clark, A.L., Bangen, K.J., Sorg, S.F., Schiehser, D.M., Evangelista, N.D., McKenna, B., Liu, T.T., Delano-Wood, L., 2017. Dynamic association between perfusion and white matter integrity across time since injury in Veterans with history of TBI. Neuroimage Clin. 14, 308–315.

Cloots, R.J., Gervaise, H.M., van Dommelen, J.A., Geers, M.G., 2008. Biomechanics of traumatic brain injury: influences of the morphologic heterogeneities of the cerebral cortex. Ann. Biomed. Eng. 36, 1203–1215.

Curry, B.D., Bain, J.L., Yan, J.G., Zhang, L.L., Yamaguchi, M., Matloub, H.S., Riley, D.A., 2002. Vibration injury damages arterial endothelial cells. Muscle Nerve 25, 527–534.

Curry, B.D., Govindaraju, S.R., Bain, J.L., Zhang, L.L., Yan, J.G., Matloub, H.S., Riley, D.A., 2005. Nifedipine pretreatment reduces vibration-induced vascular damage. Muscle Nerve 32, 639–646.

Donohew, B.E., Griffin, M.J., 2004. Motion sickness: effect of the frequency of lateral oscillation. Aviat. Space Environ. Med. 75, 649–656.

Gardner, R.C., Byers, A.L., Barnes, D.E., Li, Y., Boscardin, J., Yaffe, K., 2018. Mild TBI and risk of Parkinson disease: a chronic effects of neurotrauma consortium study. Neurology 90, e1771–e1779.

Ge, Y., Patel, M.B., Chen, Q., Grossman, E.J., Zhang, K., Miles, L., Babb, J.S., Reaume, J., Grossman, R.I., 2009. Assessment of thalamic perfusion in patients with mild traumatic brain injury by true FISP arterial spin labelling MR imaging at 3T. Brain Inj. 23, 666–674.

Gevins, A., Cutillo, B., 1993. Spatiotemporal dynamics of component processes in human working memory. Electroencephalogr. Clin. Neurophysiol. 87, 128–143.

Gordon, E.M., Laumann, T.O., Marek, S., Raut, R.V., Gratton, C., Newbold, D.J., Greene, D.J., Coalson, R.S., Snyder, A.Z., Schlaggar, B.L., Petersen, S.E., Dosenbach, N.U.F., Nelson, S.M., 2020. Default-mode network streams for coupling to language and control systems. Proc. Natl. Acad. Sci. U. S. A. 117, 17308–17319.

Haber, M., Amyot, F., Lynch, C.E., Sandsmark, D.K., Kenney, K., Werner, J.K., Moore, C., Flesher, K., Woodson, S., Silverman, E., Chou, Y., Pham, D., Diaz-Arrastia, R., 2021. Imaging biomarkers of vascular and axonal injury are spatially distinct in chronic traumatic brain injury. J. Cereb. Blood Flow Metab. 41, 1924–1938.

Hirad, A.A., Bazarian, J.J., Merchant-Borna, K., Garcea, F.E., Heilbronner, S., Paul, D., Hintz, E.B., van Wijngaarden, E., Schifitto, G., Wright, D.W., Espinoza, T.R., Mahon, B.Z., 2019. A common neural signature of brain injury in concussion and subconcussion. Sci. Adv. 5, eaau3460.

Howarth, H.V., Griffin, M.J., 2003. Effect of roll oscillation frequency on motion sickness. Aviat. Space Environ. Med. 74, 326–331.

Hua, Y., Lemerle, P., Ganghoffer, J.F., 2017. A two scale modeling and computational framework for vibration-induced Raynaud syndrome. J. Mech. Behav. Biomed. Mater. 71, 320–328.

Jenkinson, M., Beckmann, C.F., Behrens, T.E., Woolrich, M.W., Smith, S.M., 2012. Fsl. Neuroimage 62, 782–790.

Jones, M., Hewson-Stoate, N., Martindale, J., Redgrave, P., Mayhew, J., 2004. Nonlinear coupling of neural activity and CBF in rodent barrel cortex. Neuroimage 22, 956–965.

Joseph, J.A., Griffin, M.J., 2007. Motion sickness from combined lateral and roll oscillation: effect of varying phase relationships. Aviat. Space Environ. Med. 78, 944–950.

Laksari, K., Kurt, M., Babaee, H., Kleiven, S., Camarillo, D., 2018. Mechanistic insights into human brain impact dynamics through modal analysis. Phys. Rev. Lett. 120, 138101.

Liang, X., Zou, Q., He, Y., Yang, Y., 2013. Coupling of functional connectivity and regional cerebral blood flow reveals a physiological basis for network hubs of the human brain. Proc. Natl. Acad. Sci. U. S. A. 110, 1929–1934.

Lin, C.M., Tseng, Y.C., Hsu, H.L., Chen, C.J., Chen, D.Y., Yan, F.X., Chiu, W.T., 2016. Arterial spin labeling perfusion study in the patients with subacute mild traumatic brain injury. PLoS One 11, e0149109.

Liu, F., Zhuo, C., Yu, C., 2016a. Altered cerebral blood flow covariance network in schizophrenia. Front. Neurosci. 10.

Liu, K., Li, B., Qian, S., Jiang, Q., Li, L., Wang, W., Zhang, G., Sun, Y., Sun, G., 2016b. Mental fatigue after mild traumatic brain injury: a 3D-ASL perfusion study. Brain Imaging Behav. 10, 857–868.

McGarry, M.D., Van Houten, E.E., Perriñez, P.R., Pattison, A.J., Weaver, J.B., Paulsen, K.D., 2011. An octahedral shear strain-based measure of SNR for 3D MR elastography. Phys. Med. Biol. 56, N153–N164.

Meier, T.B., Bellgowan, P.S., Singh, R., Kuplicki, R., Polanski, D.W., Mayer, A.R., 2015. Recovery of cerebral blood flow following sports-related concussion. JAMA Neurol. 72, 530–538.

Militana, A.R., Donahue, M.J., Sills, A.K., Solomon, G.S., Gregory, A.J., Strother, M.K., Morgan, V.L., 2016. Alterations in default-mode network connectivity may be influenced by cerebrovascular changes within 1 week of sports related concussion in college varsity athletes: a pilot study. Brain Imaging Behav. 10, 559–568.

Murdin, L., Golding, J., Bronstein, A., 2011. Managing motion sickness. BMJ 343, d7430.

Owen, A.M., McMillan, K.M., Laird, A.R., Bullmore, E., 2005. N-back working memory paradigm: a meta-analysis of normative functional neuroimaging studies. Hum. Brain Mapp. 25, 46–59.

Palmer, R.A., Collin, J., 1993. Vibration white finger. Br. J. Surg. 80, 705–709.

Peng, S.P., Li, Y.N., Liu, J., Wang, Z.Y., Zhang, Z.S., Zhou, S.K., Tao, F.X., Zhang, Z.X., 2016. Pulsed arterial spin labeling effectively and dynamically observes changes in cerebral blood flow after mild traumatic brain injury. Neural. Regen. Res. 11, 257–261.

Pfefferbaum, A., Chanraud, S., Pitel, A.L., Müller-Oehring, E., Shankaranarayanan, A., Alsop, D.C., Rohlfing, T., Sullivan, E.V., 2011. Cerebral blood flow in posterior cortical nodes of the default mode network decreases with task engagement but remains higher than in most brain regions. Cereb. Cortex 21, 233–244.

Qiu, S., He, Z., Wang, R., Li, R., Zhang, A., Yan, F., Feng, Y., 2021. An electromagnetic actuator for brain magnetic resonance elastography with high frequency accuracy. NMR Biomed. e4592.

Raichle, M.E., 2015. The brain's default mode network. Annu. Rev. Neurosci. 38, 433–447.

Smith, S.M., 2002. Fast robust automated brain extraction. Hum. Brain Mapp. 17, 143–155.

Smith, S.M., Jenkinson, M., Woolrich, M.W., Beckmann, C.F., Behrens, T.E., Johansen-Berg, H., Bannister, P.R., De Luca, M., Drobnjak, I., Flitney, D.E., Niazy, R.K., Saunders, J., Vickers, J., Zhang, Y., De Stefano, N., Brady, J.M., Matthews, P.M., 2004. Advances in functional and structural MR image analysis and implementation as FSL. Neuroimage 23 (Suppl 1), S208–S219.

Smith, S.M., Nichols, T.E., 2009. Threshold-free cluster enhancement: addressing problems of smoothing, threshold dependence and localisation in cluster inference. Neuroimage 44, 83–98.

Steinman, J., Cahill, L.S., Koletar, M.M., Stefanovic, B., Sled, J.G., 2019. Acute and chronic stage adaptations of vascular architecture and cerebral blood flow in a mouse model of TBI. Neuroimage 202, 116101.

Stovell, M.G., Mada, M.O., Carpenter, T.A., Yan, J.L., Guilfoyle, M.R., Jalloh, I., Welsh, K.E., Helmy, A., Howe, D.J., Grice, P., Mason, A., Giorgi-Coll, S., Gallagher, C.N., Murphy, M.P., Menon, D.K., Hutchinson, P.J., Carpenter, K.L., 2020. Phosphorus spectroscopy in acute TBI demonstrates metabolic changes that relate to outcome in the presence of normal structural MRI. J. Cereb. Blood Flow Metab. 40, 67–84.

Stoyneva, Z., Lyapina, M., Tzvetkov, D., Vodenicharov, E., 2003. Current pathophysiological views on vibration-induced Raynaud's phenomenon. Cardiovasc. Res. 57, 615–624.

Tagge, C.A., Fisher, A.M., Minaeva, O.V., Gaudreau-Balderrama, A., Moncaster, J.A., Zhang, X.L., Wojnarowicz, M.W., Casey, N., Lu, H., Kokiko-Cochran, O.N., Saman, S., Ericsson, M., Onos, K.D., Veksler, R., Senatorov Jr, V.V., Kondo, A., Zhou, X.Z., Miry, O., Vose, L.R., Gopaul, K.R., Upreti, C., Nowinski, C.J., Cantu, R.C., Alvarez, V.E., Hildebrandt, A.M., Franz, E.S., Konrad, J., Hamilton, J.A., Hua, N., Tripodis, Y., Anderson, A.T., Howell, G.R., Kaufer, D., Hall, G.F., Lu, K.P., Ransohoff, R.M., Cleveland, R.O., Kowall, N.W., Stein, T.D., Lamb, B.T., Huber, B.R., Moss, W.C., Friedman, A., Stanton, P.K., McKee, A.C., Goldstein, L.E., 2018. Concussion, microvascular injury, and early tauopathy in young athletes after impact head injury and an impact concussion mouse model. Brain 141, 422–458.

Tzourio-Mazoyer, N., Landeau, B., Papathanassiou, D., Crivello, F., Etard, O., Delcroix, N., Mazoyer, B., Joliot, M., 2002. Automated anatomical labeling of activations in SPM using a macroscopic anatomical parcellation of the MNI MRI single-subject brain. Neuroimage 15, 273–289.

Wang, Y., Nencka, A.S., Meier, T.B., Guskiewicz, K., Mihalik, J.P., Alison Brooks, M., Saykin, A.J., Koch, K.M., Wu, Y.C., Nelson, L.D., McAllister, T.W., Broglio, S.P., McCrea, M.A., 2019. Cerebral blood flow in acute concussion: preliminary ASL findings from the NCAA-DoD CARE consortium. Brain Imaging Behav. 13, 1375–1385.

Wang, Y., West, J.D., Bailey, J.N., Westfall, D.R., Xiao, H., Arnold, T.W., Kersey, P.A., Saykin, A.J., McDonald, B.C., 2015. Decreased cerebral blood flow in chronic pediatric mild TBI: an MRI perfusion study. Dev. Neuropsychol. 40, 40–44.

Ware, D., Dolui, S., Duda, J., Gaggi, N., Choi, R., Detre, J., Whyte, J., Diaz-Arrastia, R., Kim, J.J., 2020. Relationship of cerebral blood flow to cognitive function and recovery in early chronic traumatic brain injury. J. Neurotrauma 37, 2180–2187.

Warren, D.E., Power, J.D., Bruss, J., Denburg, N.L., Waldron, E.J., Sun, H., Petersen, S.E., Tranel, D., 2014. Network measures predict neuropsychological outcome after brain injury. Proc. Natl. Acad. Sci. U. S. A. 111, 14247–14252.

Weech, S., Moon, J., Troje, N.F., 2018. Influence of bone-conducted vibration on simulator sickness in virtual reality. PLoS One 13, e0194137.

Winkler, A.M., Ridgway, G.R., Douaud, G., Nichols, T.E., Smith, S.M., 2016. Faster permutation inference in brain imaging. Neuroimage 141, 502–516.

Woolrich, M.W., Jbabdi, S., Patenaude, B., Chappell, M., Makni, S., Behrens, T., Beckmann, C., Jenkinson, M., Smith, S.M., 2009. Bayesian analysis of neuroimaging data in FSL. Neuroimage 45, S173–S186.

Yan, C.G., Wang, X.D., Zuo, X.N., Zang, Y.F., 2016. DPABI: data processing & analysis for (Resting-State) brain imaging. Neuroinformatics 14, 339–351.

Ye, Y., Griffin, M.J., 2014. Relation between vibrotactile perception thresholds and reductions in finger blood flow induced by vibration of the hand at frequencies in the range 8-250Hz. Eur. J. Appl. Physiol. 114, 1591–1603.

Yeo, B.T., Krienen, F.M., Sepulcre, J., Sabuncu, M.R., Lashkari, D., Hollinshead, M., Roffman, J.L., Smoller, J.W., Zollei, L., Polimeni, J.R., Fischl, B., Liu, H., Buckner, R.L., 2011. The organization of the human cerebral cortex estimated by intrinsic functional connectivity. J. Neurophysiol. 106, 1125–1165.

Yeshurun, Y., Nguyen, M., Hasson, U., 2021. The default mode network: where the idiosyncratic self meets the shared social world. Nat. Rev. Neurosci. 22, 181–192.

Yu, M., Linn, K.A., Shinohara, R.T., Oathes, D.J., Cook, P.A., Duprat, R., Moore, T.M., Oquendo, M.A., Phillips, M.L., McInnis, M., Fava, M., Trivedi, M.H., McGrath, P., Parsey, R., Weissman, M.M., Sheline, Y.I., 2019. Childhood trauma history is linked to abnormal brain connectivity in major depression. Proc. Natl. Acad. Sci. U. S. A. 116, 8582–8590.

Zwergal, A., Dieterich, M., 2020. Vertigo and dizziness in the emergency room. Curr. Opin. Neurol. 33, 117–125.